



UNIVERSITÀ  
DEGLI STUDI  
FIRENZE

## FLORE

# Repository istituzionale dell'Università degli Studi di Firenze

### **Design and simulation of a small polygeneration plant cofiring biomass and natural gas in a dual combustion micro gas turbine**

Questa è la Versione finale referata (Post print/Accepted manuscript) della seguente pubblicazione:

*Original Citation:*

Design and simulation of a small polygeneration plant cofiring biomass and natural gas in a dual combustion micro gas turbine (BIO\_MGT) / G.Riccio; Chiaramonti D.. - In: BIOMASS & BIOENERGY. - ISSN 0961-9534. - STAMPA. - 33:(2009), pp. 1520-1531. [10.1016/j.biombioe.2009.07.021]

*Availability:*

The webpage <https://hdl.handle.net/2158/395056> of the repository was last updated on

*Published version:*

DOI: 10.1016/j.biombioe.2009.07.021

*Terms of use:*

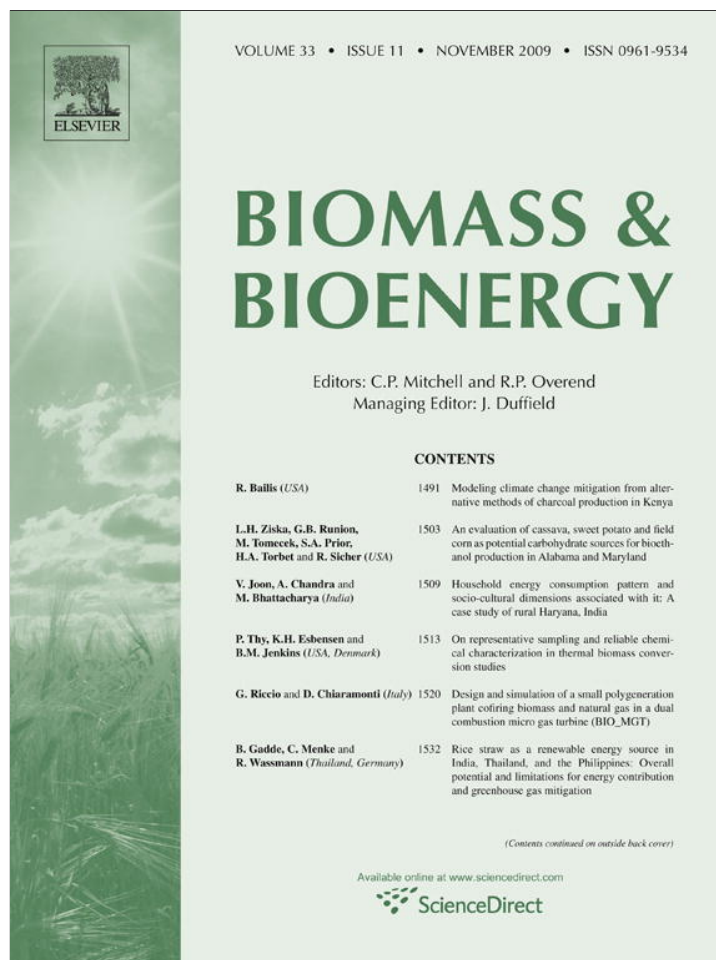
Open Access

La pubblicazione è resa disponibile sotto le norme e i termini della licenza di deposito, secondo quanto stabilito dalla Policy per l'accesso aperto dell'Università degli Studi di Firenze (<https://www.sba.unifi.it/upload/policy-oa-2016-1.pdf>)

*Publisher copyright claim:*

La data sopra indicata si riferisce all'ultimo aggiornamento della scheda del Repository FloRe - The above-mentioned date refers to the last update of the record in the Institutional Repository FloRe

(Article begins on next page)



This article appeared in a journal published by Elsevier. The attached copy is furnished to the author for internal non-commercial research and education use, including for instruction at the authors institution and sharing with colleagues.

Other uses, including reproduction and distribution, or selling or licensing copies, or posting to personal, institutional or third party websites are prohibited.

In most cases authors are permitted to post their version of the article (e.g. in Word or Tex form) to their personal website or institutional repository. Authors requiring further information regarding Elsevier's archiving and manuscript policies are encouraged to visit:

<http://www.elsevier.com/copyright>

Available at [www.sciencedirect.com](http://www.sciencedirect.com)<http://www.elsevier.com/locate/biombioe>

# Design and simulation of a small polygeneration plant cofiring biomass and natural gas in a dual combustion micro gas turbine (BIO\_MGT)

G. Riccio\*, D. Chiaramonti

Energetics Department "S. Stecco", Faculty of Mechanical Engineering, University of Florence, Via S. Marta 3, I-50139 Florence, Italy

## ARTICLE INFO

### Article history:

Received 1 April 2008  
 Received in revised form  
 16 July 2009  
 Accepted 26 July 2009  
 Published online 1 September 2009

### Keywords:

Small scale power biomass plant  
 Micro gas turbine  
 Matching analysis  
 Polygeneration

## ABSTRACT

The operation and performances of an innovative small scale polygeneration system (BIO\_MGT), which combines biomass and natural gas in a micro gas turbine, has been simulated in the present work by means of a thermodynamic matching analysis. The BIO\_MGT unit matches an externally fired cycle with a commercial Micro Gas Turbine (MGT, 100 kW<sub>e</sub>). A significant share of the total energy input (~70%) is supplied by solid biomass: the remaining is provided by natural gas. The system is therefore characterised by a dual combustion system. The configuration of the plant has been conceived so to require only minor modifications to conventional MGTs and biomass furnaces available on the market. This paper describes the design of the proposed bioenergy plant as well as the structure and the application of the in-house developed simulation model AMOS which has been used as computer-aid design tool. The design activity compared various plant schemes available from literature or past research works. The thermodynamic matching analysis of the selected configuration was then carried out, with the aim to verify compressor and turbine working points and to compare these with those typical of the MGT working under standard natural gas conditions. The steady-state matching analysis was based on the performance maps (i.e. characteristic lines) of each component. The design specifications and operating range for main and sub-components were defined, and the BIO\_MGT performance maps were computed. Results showed that both the turbine as well as the compressor will work within the acceptable limits, and plant performances have also been calculated at part load conditions.

© 2009 Elsevier Ltd. All rights reserved.

## 1. Introduction

A large interest on alternative fuels, especially biofuels, exist for power generation in Europe as well as in USA. As regards the bioenergy sector, Gas Turbines (GTs) represent one of the most interesting possible option, thanks to their performances (in terms of electrical efficiency), low emissions, and high reliability. Nevertheless, GTs require significant modifications to become compatible with unconventional fuels as

biofuels. In this context, micro/small gas turbines are seen as very promising systems for decentralised power generation and short bioenergy chains [1].

One of the most important and critical technical issues, as regards gas turbine, is represented by fuel quality. Experiences exist with biogas (i.e. gas produced by anaerobic digestion) at both large and small scale power level: however, being biogas composed by 50–70% v/v methane, the fuel quality is not too far from standard natural gas fuel, at least in terms of calorific

\* Corresponding author. Tel.: +39 055 4796 330; fax: +39 055 4796 342.

E-mail address: [Giovanni.riccio@unifi.it](mailto:Giovanni.riccio@unifi.it) (G. Riccio).

0961-9534/\$ – see front matter © 2009 Elsevier Ltd. All rights reserved.

doi:10.1016/j.biombioe.2009.07.021

value and combustion behaviour, and therefore biogas can be well used to feed GTs. Moreover, biogas is a tar-free gas, so no major gas cleaning actions are needed for reliable use of biogas in GTs (even if cleaning steps remain anyway necessary to remove some contaminants, such as  $H_2S$ ). Small scale thermo-chemical biomass conversion processes, instead, generates low-calorific tar-rich producer gas, which must be upgraded by rather complex, expensive and energy-consuming processes, i.e. not easily applicable to small scale bioenergy systems. In addition, these processes are very sensitive to physical and chemical characteristics of the biomass used. Several different approaches have been studied and/or tested by various research groups to use biomass derived fuels in GTs, which can be summarised as follows:

1. Conversion of biomass into low-calorific producer gas through atmospheric or pressurised gasification, cleaning of the gas and direct combustion in modified GT combustion chambers [2–5].
2. Conversion of lignocellulosic biomass into liquid fuel (pyrolysis oil), and direct combustion in modified GT combustion chambers [6–8].
3. Direct combustion of liquid biofuels, as bioethanol or vegetable oil, in standard or adapted GT combustors [9].
4. Direct combustion of pulverized biomass in modified GT combustors [10,11].
5. Combustion of biomass in an external furnace, and external heating of the GT cycle working fluid (air). This thermodynamic cycle is known as Indirectly or Externally Fired Gas Turbine (EFGT).

Several projects have been developed or are currently under development on the externally - or indirectly - fired gas turbine concept in EU or abroad.

The Free University of Brussels - VUB (Belgium) studied in 1996 an EFGT system in the BINAGAS project [12]. In the configuration developed at VUB, however, biomass gasification was adopted before external combustion. The size of the GT in the BINAGAS scheme was 500 kW<sub>e</sub>. Critical issues of the BINAGAS scheme were fouling and depositions on the high temperature heat exchanger.

BTG (Enschede, The Netherlands) studied the externally fired cycle (100% biomass base) for a 250 kW<sub>e</sub> plant in the framework of an EC (AIR) supported project in 1998. Even if the MGT-based EFGT was not actually built in this research work, however a detailed evaluation of the thermodynamic cycle was carried out, and some experimental activities aimed at selecting the proper materials for the heat exchanger [13] were performed. In addition, the heat exchanger design was also developed. Five different materials were investigated, after a detailed review on fouling and corrosion of metals exposed to biomass flue gases. Three high alloy steel materials, HR-120, HR-160 and SS-310, were then selected for further investigation (i.e. two weeks testing by exposition to biomass flue gases in the temperature range 450–850 °C). HR-160 and SS-310 showed the best performances: material loss after 15 years operation was predicted assuming a parabolic law (0.2 mm for SS-310, and 0.5 mm for HR-160). SS-310 was finally selected thanks to the lower cost at that time, and a shell-and-tube heat exchanger was designed (composed by 344 tubes of 8.4 m length).

The University of British Columbia [14] analysed three different EFGT configurations for the application to typical British Columbia sawmills: the first scheme was based on metal gas/air shell-and-tube heat exchanger and a wood waste refractory-lined combustor, the second one on the same configuration but using a high temperature ceramic heat exchanger, the third one on the combination of an atmospheric fluidised bed combustor and a heat exchanger immersed in the bed followed by a gas–gas heat exchanger. Material restrictions limited the maximum air temperature achievable with the metallic heat exchanger to 650 °C. All these configurations also included the possibility of additional natural gas firing to increase the Turbine Inlet Temperature (TIT) to 1130 °C before entering the turbine, even if the use of the ceramic heat exchanger in combination with the wood waste combustor allows to achieve 1140 °C, and no additional natural gas combustion is therefore needed. The possibility of using turbine exhaust as combustion air was not considered. The study examined gas turbines from 660 kW<sub>e</sub> to 3981 kW<sub>e</sub> (and multiples of that). A linear programming model was applied to estimate economic performances.

The University of Rostock recently analysed a similar EFGT configuration at small scale, with the metallic heat exchanger tubes immersed in the bed of a fluidised bed combustor [15].

CANMET (Canada), following the previous work by the University of British Columbia [14], studied the 100% biomass indirectly fired gas turbine scheme [16] in the capacity range of 250–1000 kW<sub>e</sub>. Design inlet temperature for the heat exchanger, the most critical component of the EFGT system, was rather high (1010 °C), but details on the heat exchanger (such as materials, resistance to fouling and corrosion, etc) were not given. The GT was designed to operate at 420 kPa max pressure, and the Turbine Inlet Temperature (TIT) was 850 °C. Again, the thermal energy available in the turbine exhaust was not recuperated for biomass combustion. Economic calculations for this plant have been carried out assuming 25 years lifetime and considering both new and refurbished turbines. Electrical efficiencies were estimated in the range of 20–25%, but no thermodynamic calculation was given to detail these figures. Talbott's (UK) developed and tested (short term - total of 24 h in 4 tests with biomass) a micro gas turbine system based on the 100% externally biomass fired concept [17]. A biomass (pellet) combustor was developed by Talbott's, and TG50 produced by Bowman Power Ltd was the selected gas turbine. Waste heat from turbine exhaust flue gas was collected by modified ductwork and returned into combustion air streams. The generated energy during the experiment achieved 30 kW<sub>e</sub> power: turbine acceleration was slower than conventional gas turbine. Heat exchanger proved the principle to work, but this work concluded that extensive testing and further development is needed, lasting at least 1 year. GT regulation was a major issue. Commercial perspectives have been considered good. No measurements of emissions were carried out. Recently, Talbott's started the commercialisation of a multifuel externally fired gas turbine of 80–100 kW<sub>e</sub> and 150–200 kW<sub>th</sub> scale, anticipating an overall electrical efficiency of 20%, a consumption of 80 kg<sub>DT</sub> h<sup>-1</sup> and 8000 h per year availability [18].

Other research groups studied and are still studying the biomass-fed EFGT concept, among which: the Technical



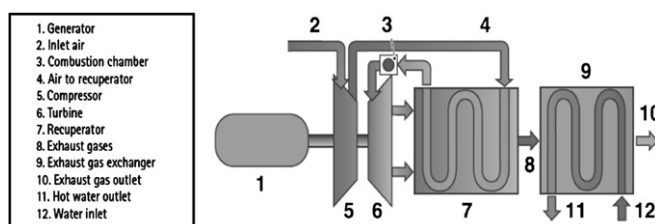


Fig. 2 – Regenerative Cycle and main component for a typical MGT (courtesy by Turbec).

The Heat Exchanger (HE) is a crucial component of the system which has to withstand aggressive biomass flue gas streams at high temperatures ( $\sim 850\text{--}900\text{ }^{\circ}\text{C}$ ) and, at the same time, around 400 kPa differential pressure. The HE specifications have been derived from scientific and technical literature [13,22,23]. Taking into account these requirements, a metallic one-pass shell-and-tube heat exchanger with one stationary head and one floating head has been selected as the most suitable one. The HE is designed to exchange about  $500\text{ kW}_{\text{th}}$ : tube length and shell diameter are approximately 8 m and 1 m respectively.

The biofurnace fuel energy input is around  $350\text{ kW}_{\text{th}}$ . The special requirement for this component is given by the use of the turbine exhaust as combustion air, limiting the EGR (Exhaust Gas Recirculation) flow rate, and to perform efficient combustion. High reliability, low emissions (CO, CxHy, NOx, particulate), low investment, low operating and maintenance costs are additional requirements. After having evaluated different combustion systems, the underfeed stoker furnace type has finally been selected.

The development of a suitable control system (CS) also plays a major role to achieve a proper and safe plant operation: it has to be fully compatible with both the MGT as well as the Biofurnace control systems, and match the constraints given by the heat exchanger and the biofurnace in terms of ramp load and thermal inertia. The plant is equipped by a valve posed at the biofurnace outlet to by-pass the heat exchanger: in case of load break-down, the control system interrupt the fuel supply (natural gas and biomass) by opening the by-pass valve, so to avoid MGT over speed. The main control system consists of

a central control unit processing signals received from both the MGT and the biofurnace control systems, as well as from other controls and measurements distributed along the entire plant (mainly actuators, valves, fans, thermocouples, pressure transducers). A simple scheme of the Bio\_MGT main control system is given below (Fig. 4).

## 2. Materials and methods

### 2.1. The matching analysis model

A steady-state thermodynamic matching analysis of the system has been performed by developing and applying the AMOS (*Advanced MGT System Operation Simulator*) code: in fact, a typical matching procedure among rotating and stationary elements allows to estimate the plant behaviour along the whole operating domain and thermodynamic cycle [24]. The matching analysis allows to perform a more realistic calculation of the plant performances, especially when considering off-design conditions induced by either thermal or mechanical load changes. In the present work this kind of analysis aims at verifying the technical feasibility of matching commercial components (i.e. without implementing major modifications on them) into a new configuration, giving special attention to rotating parts. In particular, the critical issue to be checked is whether the MGT working points still remain acceptable when the turbomachine is integrated into the Bio\_MGT EFGT scheme, characterised by different pressure loss and operating conditions. The AMOS code Fig. 5 is

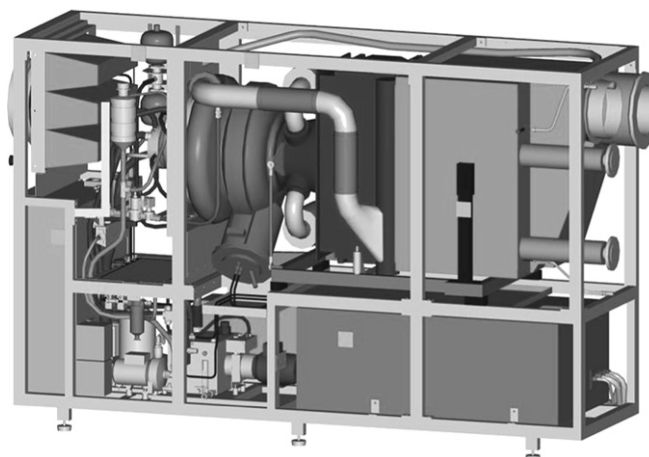


Fig. 3 – The MGT Turbec T100 (courtesy by Turbec).

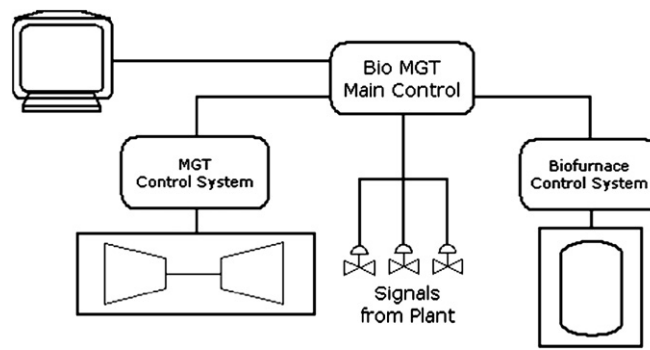


Fig. 4 - Scheme of Main Control and Monitoring system.

a simulation tool written in Fortran language, developed at the Energetic Department of the University of Florence. The code, based on black box model, is able to simulate different plant configurations based on MGTs. Each component behaviour is implemented (as external database) in the code by means of its characteristic curves. The gas properties (specific heat values) are computed as function of the gas composition ( $N_2$ ,  $O_2$ ,  $CO_2$ ,  $H_2O$ ) and temperature at each node of the system by means of correlations taking into account the heat specific value temperature variation [25,26].

The design and off-design computations have been carried out by using radial-flow turbine and compressor maps (rotating components). The internal recuperator, the combustion chamber and the heat exchanger pressure losses are calculated as linear variation with the flow rate [27], for which performance maps (also known as “characteristic lines”) are also available. The algorithm implements an iterative procedure: the main loop follows an iterative calculation initialised by a first attempt on the mass flow rate elaborated by the compressor at a given rotational speed. The pressure ratio and the efficiency of the compression process are calculated from the compressor performance maps by means of an interpolation algorithm. The same pressure ratio, reduced by the pressure losses, is considered for the turbine expansion that is the input value to compute the mass flow rate and the expansion efficiency through the turbine performance maps. The iterative procedure is repeated until the compressor flow rate becomes consistent with the one elaborated by the turbine (considering, if present, the addition of

the fuel as well). The algorithm usually achieves convergence in about 10–15 iterations.

The closure condition of the matching model is obtained by assuming that the discharge pressure becomes equal to the sum of the ambient pressure and the pressure losses through the components (mainly pipes, heat exchanger, biofurnace) between the turbine outlet and the exhaust chimney.

The main input data are operational as well as performance parameters: the rotational speed, the turbine inlet temperature (TIT), the biofurnace exhaust gas outlet temperature (i.e. heat exchanger inlet hot flow temperature), the heat exchanger effectiveness ( $\epsilon = Q/Q_{max} = T_{out-cold} - T_{in-cold} / T_{in-hot} \times T_{in-cold}$ ), the electrical losses, and the composition of the fuel gas and the biomass.

In particular, the heat exchanger (HE) effectiveness  $\epsilon$  is assumed as a constant value over the whole operating range. Since the HE effectiveness has a significant influence on the regenerative GT cycles performances, this assumption has been carefully verified, in particular by comparing the 100% and the 50% load conditions. The effectiveness is a function of the heat transfer area number (NTU, as defined below), the capacity rate ratio ( $C^*$ ) and the heat exchanger geometry:

$$\epsilon = f(NTU, C^*, \text{geometry})$$

As the geometry does not change (the heat exchanger geometry is kept the same) in the considered cases, and since the  $C^*$  variation (partial load) is of minor importance (the cold

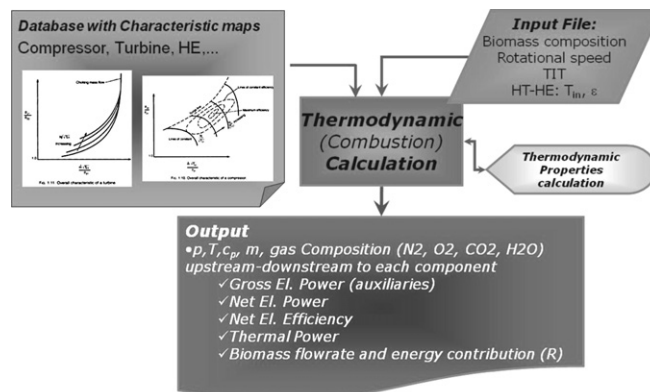


Fig. 5 - AMOS Model main block Diagram.

and hot side mass flow rate ratio is almost constant, close to the unit for each load condition), changes are only related to the different mass flow rates. Therefore  $\varepsilon$  depends only by the NTU parameter, which is defined as:

$$NTU = UA/C_{min}$$

where the global heat exchange coefficient  $U$  is assumed equal to the mean value over the whole heat exchanger. As  $A$  remains unchanged, the NTU variation only depends on  $U$  and the minimum heat capacity rate  $C_{min}$  variations (where  $C_{min} = m \cdot c_p$  air side). The global thermal exchange coefficient mainly depends on the internal and external convection heat exchange coefficients  $h_i$  and  $h_o$  (where subscripts “i” and “o” refer to tube internal and external/outer flows). In order to calculate  $h_i$  and  $h_o$ , the Nu (Nusselt number) can be used, with:

$$Nu = f(Re, Pr)$$

The inner side Nu can be evaluated by using the correlation suggested by Zakauskas [28], while the outer one by that given by Kern [29]. Results of the calculation lead to the NTU evaluation. Considering a load change from 100% to 50% of the plant nominal value, and evaluating  $k$  and  $c_p$  by air standard data at the mean temperature between inlet and outlet sections, NTU changes from 2.9 to 2.4 from full to 50% load, thus decreasing by  $\sim 17\%$ . Moreover, being the HT-HE a shell & tubes one, the efficiency becomes rather independent [30] from the NTU value if  $NTU > 2$  and  $C^* \sim 1$ . In conclusion, the assumption of maintaining the heat exchanger efficiency ( $\varepsilon$ ) constant over the operational range is a proper one.

The Biofurnace is modelled as a black box with three governing equations: mass balance equation, energy balance equation and EGR characteristic equation of the biofurnace based on experiments as well as combustion calculation [31].

$$m_{EGR} = k * m_{bio} \text{ where } k = f(\%moist.; \lambda_{pZ})$$

The biomass air stoichiometric ratio as well as the lower calorific value are computed from the composition and moisture content of the biomass. The model also considers the possibility to burn in the MGT combustion chamber a general gaseous fuel composed by the following main species:  $CH_4$ ,  $H_2$ ,  $CO$ ,  $CO_2$ ,  $N_2$ ,  $H_2O$ . The fuel gas air stoichiometric ratio as well as its LHV are computed from the fuel gas volume composition.

The validation of the model was carried out by evaluating the capability of the algorithm to reproduce and correctly interpolate the performance maps of the rotating parts at each allowed rotational speed and simulating reference test-cases, among these the MGT in standard configuration fired by methane.

Results of the calculation give inlet and outlet thermodynamic working conditions (temperature, pressure, gas composition, heat specific value) for each component. The performances, the working points as well as the design specifications for each component are then computed.

The main output from the calculation are the gross and net electric power, the fuel consumption (in terms of both natural

gas and biomass flow rate), and the biomass energy contribution  $R$ , defined as:

$$R = m_{Bio} \cdot LCV_{Bio} / (m_{Bio} \cdot LCV_{Bio} + m_{CH_4} \cdot LCV_{CH_4})$$

## 2.2. Assumptions for the calculations

The definition of the input for the calculations were obtained from the data sheet provided by the manufacturer [21] and from literature. As previously reported, the model also needs the characteristic lines of each component (compressor, turbine and pressure losses lines for the static components) as input to the computation. Amongst the main input parameters, the mechanical efficiency  $\eta_{mec}$  was assumed equal to 0.99, thus obtaining a total figure for the mechanical losses at full load of  $\sim 4.0 \text{ kW}_e$ , in agreement with literature [32]. Kays effectiveness for the internal recuperator has been estimated equal to 89%, as suggested by the reference literature [24,27,32]. The recuperator characteristic line has been estimated from the work by Svenska Rekuperator AB [33]. These curves do not take into account the pressure loss increase due to the connecting pipes between the recuperator and the microturbine. For this reason, the pressure losses (obtained from the above mentioned curve) have been increased by an additional term [32,34–36]. The electrical losses are dominated by power electronics dissipation, which is roughly constant (about 10–12  $\text{kW}_e$ ) all over the power range [34].

The pressure loss on the gas-side of the thermal user recovery unit was evaluated from manufacturer technical data, and assumed equal to 200 Pa.

The simulation of the BIO\_MGT plant has been performed considering the following main assumptions: Kays effectiveness ( $\varepsilon$ ) for the HT-HE equal to 0.89, biofurnace exhaust gas temperature equal to 880 °C, biofurnace primary zone excess air ratio  $\lambda$  equal to 0.6, exhaust flow gas temperature at the chimney 180 °C (also exhaust gas recirculation temperature). The EGR flow rate has been computed as a function of the biomass moisture content and corrected with the combustion air temperature according to the equation already given. The considered biomass composition is given in Table 2.

## 3. Results and discussion

The model has initially been used to simulate the standard MGT plant in its original configuration, as described in Fig. 2 (MGT fed with natural gas, no biomass and external combustion). AMOS has then been applied to calculate the Bio\_MGT system (Fig. 1). The standard MGT characterisation not only represents a mean for validating the AMOS code, but also gives the reference case for the BIO\_MGT system.

### 3.1. Simulation of the standard MGT system

Table 1 shows the performance parameter computed for the original MGT fired by natural gas at design working condition and fixed rotational speed ( $\sim 69,000 \text{ RPM}$ ). These results are in good agreement with the nominal values, and therefore validate the AMOS solver.

**Table 1 – Standard MGT nominal performances at design point vs. computed values (ISO standard conditions).**

MGT Performance Parameter		Nominal values	Computed values
Gross Electric Power	kW	–	110.6
Net Electric Power	kW	100 (+3)	104
User Thermal Power (hot water) exhaust down to 70 °C	kW	155 (+5)	159.8
Maximum temperature for thermal recovery	°C	270	264
Net electrical efficiency	$\eta_{el}$	30 (+1)	31.1
Thermal recovery efficiency	–	–	47.8
Compression ratio	B	~4,5	4.26
Exhaust gas flow rate	$g\ s^{-1}$	800	780
Natural gas/methane mass flow rate	$g\ s^{-1}$	6.6	6.7
Thermal power exchanged at the regenerator	kW	–	335.3

The MGT can be controlled by regulating both the rotational speed (i.e. flow rate) and by modifying the turbine inlet temperature (TIT). Calculations were performed for each condition in order to reproduce the performance map of the MGT.

Fig. 6 shows the original MGT performance map (net electric power vs. net electric efficiency) in non-dimensional form with respect to the nominal condition. The map summarizes the MGT working points, highlighting the lines with constant TIT and those with constant rotational speed, i.e. about constant air flow rate. It can be observed that the maximum net electrical efficiency does not correspond to the maximum net electric power, that defines the design point. This behaviour remains unchanged at each TIT values. Assuming a fixed value for the rotational speed, both the efficiency and the power increase with TIT. In case of “very low” rotational speed (i.e. <40,000 rpm), the TIT influence becomes smaller on the machine performances, and the lines tend to collapse into a single point. It has to be remarked that for power loads above 50% of the nominal load, the efficiency lines for a fixed TIT value become rather flat: this identifies a wide working range characterised by smooth variation of the efficiency. However, in some applications and probably also in the case of BIO\_MGT, it could be necessary to operate the MGT at fixed rotational speed. In this case the regulation is performed by varying the TIT. At this control mode corresponds a steep efficiency reduction at partial load.

**Table 2 – Biomass Composition.**

Component	Ccontent (w/w, db)
Carbon	0.500
Hydrogen	0.060
Oxygen	0.4257
Nitrogen	0.004
Sulfur	0.0003
Ash	0.010
moisture (tot w.b.)	0.35

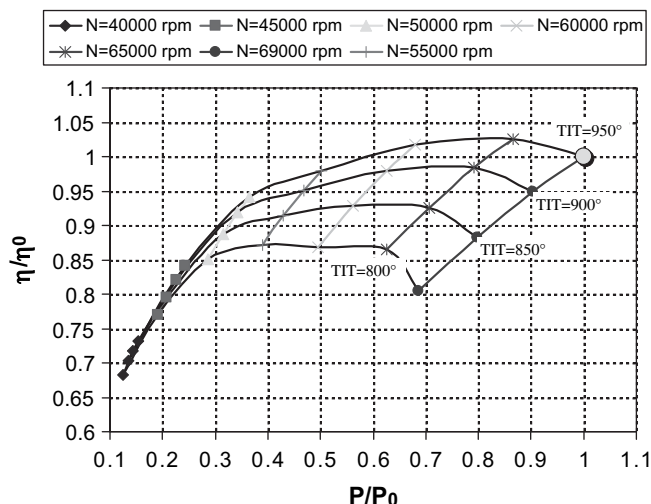


**Fig. 6 – MGT non-dimensional performance map; net electric efficiency vs. net electric power.**

### 3.2. Simulation of the BIO\_MGT system

The results of the calculation at design condition (ISO standard condition) are given in Table 3. As regards the performances at design point, the electrical net power remains approximately the same as the standard (natural gas) MGT, while the electrical efficiency decreases by about 8 basis points. The recoverable thermal energy at ~360 °C is slightly increased, from approx. 155 to 168 kWth, due to the increase in the mass flow rate and the higher exhaust temperature, from 270 to 358 °C. A very important results is represented by the

**Table 3 – Computed BIO\_MGT performances at design point (ISO standard conditions).**

BIO_MGT Performance Parameter		Computed values
Gross Electric Power	kW	114.6
Net Electric Power	kW	101.6
User Thermal Power (hot water) exhaust to 180 °C	kW	168.2
Maximum temperature for thermal recovery	°C	358
Thermal power exchanged at the HT-HE	kW	521
Net electrical efficiency $\eta_{el}$	–	21.9
Thermal recovery efficiency, $\eta_{th}$	–	36.2
Compression ratio, $\beta$	–	4.24
Exhaust gas flow rate	$g\ s^{-1}$	812
Natural gas/methane mass flow rate	$g\ s^{-1}$	2.8
Biomass mass flow rate	$g\ s^{-1}$	28.5
Biomass fuel energy input	kW	323.4
Biomass Energy Contribution	%	69.5

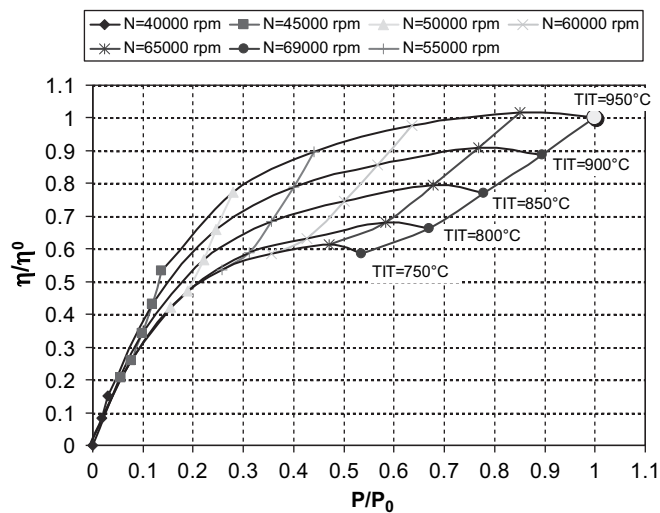


Fig. 7 – BIO\_MGT non-dimensional performance maps.

biomass energy contribution, that reaches around 70% of the primary energy fed to the system.

The whole BIO\_MGT performances map (Fig. 7) shows only minor differences with respect to the standard (i.e. natural gas fed) MGT map, so that similar remarks can be made for the BIO\_MGT configuration. The regulation performed by varying the rotational speed at constant TIT guarantees for higher efficiency over a wide load operating range.

The influence of the high temperature gas-gas heat exchanger (HT-HE) design specification on the plant performances was also evaluated. Simulation were repeated considering a more conservative working conditions for the HT-HE: inlet hot gas temperature limited to 850 °C and effectiveness equal to 0.84, corresponding to air preheating up to 750°. Material thermal stresses are reduced in this way, and the heat exchanger length is slightly reduced. Results of the calculations, at full-load operation, show that power remains about the same (~ 101 kW<sub>e</sub>): the advantage from a very small increase in turbine mass flow rate is compensated by the increase in fuel gas compressor energy consumption. The net electrical efficiency shows a small increase (~ +1%) since the share of natural gas internal combustion also increases. The biomass energy contribution is instead reduced to approximately 59%.

The biomass energy contribution is a function of the rotational speed and the TIT (Fig. 8). The biomass energy contributions decreases with the rotational speed at constant TIT: this trend will not be observed if R is close to 1. At nominal TIT, the biomass energy contribution R grows from 0.60 (at 45% load and 45,000 rpm) to 0.70 (full-load conditions). By operating the system at a lower TIT, the biomass energy contribution is increased, but at the same time the system electrical efficiency is reduced. If the TIT is set equal to or below 800 °C, the Bio\_MGT plant becomes “fully green” with a design net electric efficiency around 15%, and a net electric power of 67 kW<sub>e</sub>. Operating the plant by external combustion only does not allow to achieve sufficiently high temperatures at the turbine inlet, since the HE hot-side temperature has to be kept below 900 °C for material and cost reasons, determining therefore a TIT significantly lower than the design one.

Summarising, the main results of the model show that the BIO\_MGT plant can properly work in the dual combustion mode, respecting the operational range of each component (mainly the compressor and the turbine).

The “biomass energy use efficiency” parameter has been evaluated by adopting the following definition.

$$\eta_{el\_bio} = (P_{Net\_EL\_overall} - 0.30 * P_{In\_CH_4}) / P_{In\_Biomass}$$

The BIO\_MGT system is able to convert about 21.8% of the entire fuel energy input into electrical power. The chemical energy in the natural gas is usually converted into electricity in a standard MGT at significantly higher efficiencies. A figure of 22% is interesting only for small scale bioenergy systems, since natural gas micro gas turbines of similar size (around 100 kW) normally achieve 28–30% electrical efficiency. However, in order to take this into account, and adopt a very conservative approach, we can assume that the same amount of natural gas fired on BIO\_MGT system could have been converted into electrical power with the same efficiency than

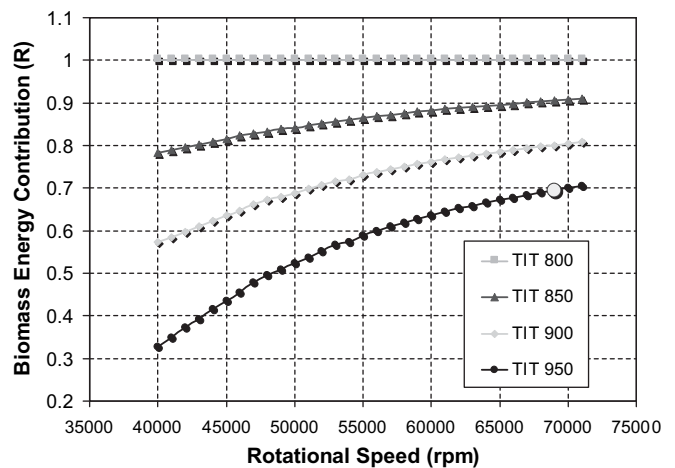


Fig. 8 – Biomass energy contribution at different working conditions, rpm and TIT.

**Table 4 – BIO\_MGT performance at design conditions vs. BIO\_MGT in 100% biomass mode and full-load conditions.**

Parameter		Cofiring	100% biomass
TIT	K	950	805
Net Electric Power	kW	101.6	68.4
Bio_MGT El. Efficiency	–	21.85	14.56
Biomass Energy contribution	–	0.695	1.00
Biomass fuel mass flow rate	g s <sup>-1</sup>	28.5	42.0
Natural Gas mass flow rate	g s <sup>-1</sup>	2.8	0.00
Energy from biomass	kW	323.4	469.6
Energy from fuel methane gas	kW	140.0	–
n(fuel methane gas)	–	30.0%	30.0%
Electric power from NG	kW	42.0	–
Electric power from biomass	kW	59.6	68.4
η (biomass)	%	18.4	14.6

the standard MGT configuration (30%). By calculating the theoretical electrical power from biomass fuel as the difference between total net electric output power and power from fuel gas at 30% efficiency, the biomass fuel conversion efficiency can be computed at 18.4% (see Table 4). Finally, it is worth to remark that by operating the Bio\_MGT in the Dual Combustion mode, a ~400 basis points increase in the biomass to power conversion efficiency can be obtained.

**3.3. Compressor and turbine working points comparison**

As expected, the microturbine operational condition will change in the BIO\_MGT configuration compared to the standard MGT. As regards the rotating components, the following diagrams (Figs. 9 and 10) show the working points on the

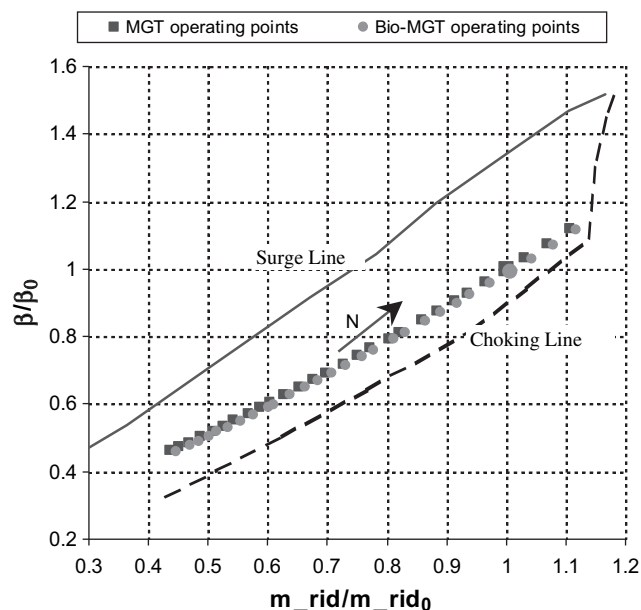


**Fig. 9 – Comparison between the compressor working point locii on the compressor map in case of MGT and BIO\_MGT configurations.**

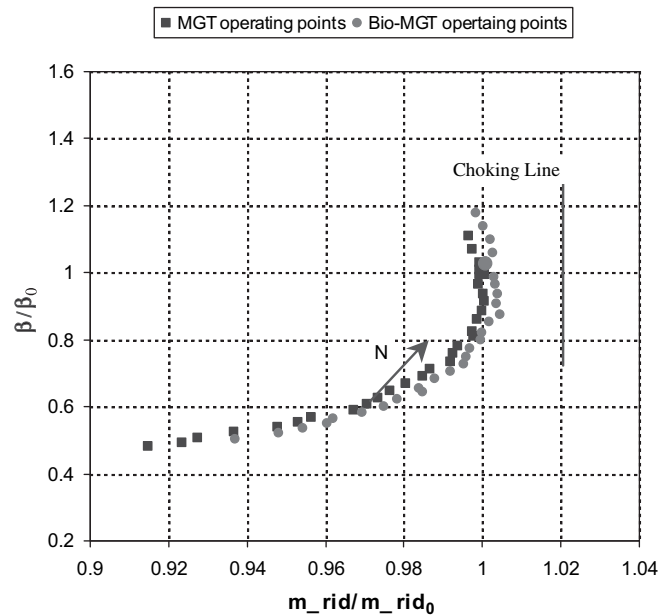


**Fig. 10 – Comparison of the turbine working point locii on the turbine map in case of MGT and BIO\_MGT configuration.**

compressor and turbine characteristic maps in case of MGT (black square) and BIO\_MGT (grey circles).

The largest point (1,1) refers to the nominal operating condition. In particular, the diagrams respectively show the compressor pressure ratio and the turbine expansion ratio related to the flow coefficient (m\_rid). For each graph the two series represent the turbine and the compressor operating points from 45,000 to 72,000 rpm (black arrows indicate the increasing rotor speed).

Both the choking line and the surge line are displayed in the compressor map: the compressor operating points lie far enough from surge and choking lines. It can also be observed how the operating points remain close to each other for the standard and the BIO\_MGT configurations: the BIO\_MGT mass flow rate is only 1% (or less) higher than the MGT one, whereas the compressor pressure ratio is 1% lower in the BIO\_MGT configuration at high rotating speed only.

The turbine graph (Fig. 10) shows the choking line: it represents an important verification mean the fact that the operating points of both configurations are rather far from this line, thus assuring that the turbine will properly work over the entire rotating speed range. The difference between the two configurations is almost negligible (from 2 to 3% at low rotational speed to 0.1–0.3% at higher rotational speed).

As regards the pressure ratio for compressor and turbine, small differences in the turbine behaviour can be observed, whereas in the compressor almost no differences between the two configurations (standard MGT vs. BIO\_MGT) exist. At lower rotational speed the turbine pressure discharge in the MGT mode decreases, since the mass flow rate and consequently the pressure loss in the regenerator and flue gas pipe also decrease (Fig. 10). In the BIO\_MGT mode the turbine pressure discharge is fixed by the operating pressure requested by the Biofurnace.

Summarising, the rotational components, compressor and turbine, of the microturbine integrated into the BIO\_MGT layout maintain operating conditions close to the standard ones. The microturbine operating points works in a safe and high efficiency area of the performance map in the BIO\_MGT system, far enough from both surge and choking line over the whole rotational speed range. In conclusion, the expected results for the BIO\_MGT cycle represent an attainable realistic goal.

As regards greenhouse gas emission savings, the CO<sub>2</sub> specific emission at the nominal condition for the original (natural gas fed) MGT is calculated at 650 g kWh<sub>e</sub><sup>-1</sup>; thanks to the combined use of natural gas and biomass fuel (which accounts for 69.5% of the energy input to the MGT) the system emissions are approximately reduced to 273 g kWh<sub>e</sub><sup>-1</sup>, i.e. 42% of the natural gas base case. Moreover, further considerations should be elaborated considering the higher amount of heat that remains available from the BIO\_MGT compared to the recoverable heat from the standard MGT (168 kW<sub>th</sub> instead of 155 kW<sub>th</sub> for the standard natural gas plant). If this is taken into account, a CO<sub>2</sub> reduction of more than 2730 g h<sup>-1</sup> can be estimated as a substitute of a traditional natural gas boiler of 210 g kWh<sub>th</sub> CO<sub>2</sub> emission (thermal efficiency assumed equal to 0.94).

#### 4. Conclusions

The research work investigated an externally fired biomass micro gas turbine system which also adopt a share of internal natural gas combustion (BIO\_MGT): the main scope of the theoretical analysis here reported was to support the final design and the component specifications for a system which has been built and is currently being assembled. A numerical model has been developed to perform the matching analysis between the various components of the plant. The code was validated by simulating the standard MGT natural gas plant, that represents the reference condition. The behaviour of both the MGT as well as the other static components (as the bio-furnace and the heat exchanger) has been simulated when operating in the new cycle and therefore under different operating conditions. The working points for both compressor and turbine have been verified, and the setting points and performances calculated. The analysis did not show considerable variations as regards the operating points for both turbine and compressor, that lie in a high efficiency operation zone and far enough from choking and surge lines, either considering in the new biomass-fed configuration-design or partial load conditions.

The performances of the BIO\_MGT plant were then calculated: the estimated net electric power is ~101.6 kW, the net electric efficiency ~21.8%, and the thermal power available for cogeneration 168.2 kW at 360 °C, with a share of biomass contribution equal to approximately 70% on energy basis. Even at 40% partial load the study confirmed the possibility to achieve reasonable performances:  $\eta/\eta_0$  between 0.6 and 0.85 depending on TIT (Fig. 7). In terms of operating mode, the calculation outlined how maintaining the TIT constant and varying the rotational speed guarantees better performances at partial load. Finally, the efficiency in biomass energy use has been calculated: considering as reference case the natural

gas MGT, which conversion efficiency is equal to 30%, the BIO\_MGT in dual combustion mode is able to achieve a biomass to electric energy conversion efficiency of 18.4%, which corresponds to ≈4 basis points improvement compared to the “fully green” (100% biomass) option.

Future work will be the experimental validation of the results presented in the present paper, through the BIO\_MGT demonstration plant that is currently under installation in Tuscany.

#### Acknowledgements

The BIO\_MGT project is supported by the European Commission DG-TREN through the Sixth Framework Programme (FP6). Authors wish to acknowledge Prof. Eng. Francesco Martelli, Director of CREAR, and the partners of the project: Turbec R&D, Graz University of Technology (TU-Graz), RNS; MAWERA-Holzfeuerungsanlagen GmbH, IFEU-Inst. für Energie und Umweltforschung Heidelberg GmbH and the Cooperative “Il Forteto”. Authors wish also to acknowledge Eng. Adriano Spadi of the Energetic Department “Sergio Stecco”, University of Florence, who collaborated to this research project.

#### REFERENCES

- [1] Obernberger I. Decentralized biomass combustion: state of the art and future development. *Biomass and Bioenergy* 1998;14(1):33–57.
- [2] Sridhar HV, Sridhar G, Dasappa S, Paul PJ, Mukunda HS. On the operation of a high pressure biomass gasifier with gas turbine. In: Maniatis K, Grimm HP, Helm P, Grassi A, editors. *Proceeding of the 15th European biomass conference & exhibition*. Berlin; 2007. p. 964–7.
- [3] Rabou LPLM, Grift JM, Conradie RE, Fransen S, Verhoeff F. Micro gas turbine operation with biomass producer gas. In: Maniatis K, Grimm HP, Helm P, Grassi A, editors. *Proceeding of the 15th European biomass conference & exhibition*. Berlin; 2007. p. 935–7.
- [4] Stahl K, Neergaard M. IGCC power plant for biomass utilisation. Värnamo, Sweden, *Biomass and Bioenergy* 1998; 15(3):205–11.
- [5] Prussi M, Riccio G, Chiaramonti D, Martelli F. Evaluation of a micro gas turbine fed by blends of biomass producer gas and natural gas. In: *Proceedings of ASME turbo expo 2008*, ASME, editor. Paper GT2008-50236.
- [6] Andrews RG, Zukowski S, Patnaik PC. Feasibility of firing an industrial gas turbine using a biomass derived fuel. In: Bridgwater AV, Boocock DGB, editors. *Developments in thermochemical biomass conversion*. London: Blackie Academic and Professional Press; 1997. p. 495–506.
- [7] Lopez Juste G, Salva Monfort JJ. Preliminary test on combustion of wood derived fast pyrolysis oils in a gas turbine combustor. *Biomass and Bioenergy* 2000;19:119–28.
- [8] Strenziok R, Hansen U, Künster H. Combustion of bio-oil in a gas turbine. In: Bridgwater AV, editor. *Progress in thermochemical biomass conversion*. Oxford: Blackwell Science; 2001. p. 1452–8.
- [9] Johansson P. Development of a dry low-NOx combustor for the VT100 automotive gas turbine. In: *Proceedings of ASME turbo expo 1997*. ASME, editor. Paper 97-GT-74.

- [10] Wingelhofer F. Directly wood particle fired gas turbine plants: concept, experimental results and potential applications for combined heat and power generation with moderate output. In: Maniatis K, Grimm HP, Helm P, Grassi A, editors. Proceeding of 15th European biomass conference & exhibition. Berlin; 2007. p. 1574–82.
- [11] Craig JD, Purvis CR. A small scale biomass fueled gas turbine engine, transactions of the ASME. Journal of Engineering for Gas Turbines and Power 1999;121:64–7.
- [12] De Ruyck J. An externally fired evaporative gas turbine cycle for small scale biomass gasification. In: Chartier P, editor. Proceeding of 9th EU conference on biomass for energy and the environment. Pergamon, Oxford; 1996.
- [13] Knoef H. The indirectly fired gas turbine for rural electricity production from biomass, Project Brochure and Reports; 1998. Contract FAIR-CT95–0291.
- [14] Evans RL, Zaradic AM. Optimization of a wood-waste-fuelled indirectly fired gas turbine cogeneration plant. Bioresource Technology 1996;57:117–26.
- [15] Vincent T, Strenziok R, Steinbrecht D. Cogeneration of electricity and heat from biogenic solid fuels in a stationary fluidised bed reactor linked with an externally fired micro gas turbine. In: ETA-WIP, editor. Proceeding of 16th European biomass conference & exhibition. Valencia; 2008. p. 1358–62.
- [16] Preto F. Small scale wood fired cogeneration in Canada: IFPG sawmill case studies. In: Proceedings of the clean air 2003 conference. Lisbon; 2003.
- [17] Pritchard D. Biomass combustion gas turbine CHP, Contract Report ETSU B/U1/00679/00/REP, 2002.
- [18] Schmid R, Gaegauf C. Biomass combined cycle: efficient solution for decentralised biomass power. In: ©2008 ETA-Renewable, editor. Proceeding of sixteenth European biomass conference & exhibition, Firenze 2008, Valencia; 2008. p. 1363–5.
- [19] Savola T, Tveit T-M, Laukkanen T. Biofuel indirectly fired microturbine state of the art. TKK, Laboratory of Energy Engineering and Environmental Protection, Espoo, [http://eny.hut.fi/research/process\\_integration/bioifgt\\_Jan.pdf](http://eny.hut.fi/research/process_integration/bioifgt_Jan.pdf); 2005.
- [20] Riccio G, Martelli F, Maltagliati S. Study of an external fired gas turbine power plant fed by solid fuel. In: Proceeding of ASME turbo expo 2000. ASME, editor. Paper 0015-GT-2000.
- [21] Turbec AB. T100 microturbine system, D12451 Technical description, 2002, Copyright © 2002 Turbec AB.
- [22] Cocco D, Deiana P, Cau G. Ottimizzazione di uno scambiatore di calore ad alta temperatura per impianti EFGT alimentati con Biomasse. In: Proceeding of the 58th Italian annual congress ATI, SGE Editoriali (ed.), Padova, vol. 1; 2003. p. 133–44.
- [23] Brunner T, Joeller M, Obernberger I, Frandsen F. Aerosol and fly ash formation in fixed bed biomass combustion systems using woody biofuels. In: ETA-WIP, editor. Proceeding of 12th European conference and technology exhibition on biomass for energy, industry and climate protection, Amsterdam; 2002. p. 685–9.
- [24] Bozza F, Tuccillo R. Transient operation analysis of a cogenerating micro-gas turbine. In: Proceedings of ESDA 2004. ASME editor. Paper ESDA 2004–58079.
- [25] Moore WJ, editor. Chimica fisica. Padova: Piccin; 1967.
- [26] Van Wylen GJ, Soontag RE. Fundamental of classic thermodynamics. New York: Wiley; 1985.
- [27] McDonald CF. Recuperator consideration for future higher efficiency microturbines. Applied Thermal Engineering 2003; 23:1463–87.
- [28] Zukauskas AA. Convective heat transfer in cross flow. In: Kakac S, Shah RK, Aung W, editors. Hand book of single-phase convection heat transfer. New York: Wiley; 1987. p. 6. 1–6.45. Chapter 6.
- [29] Kern DQ, Kraus AD, editors. Extended surface heat transfer. New York: McGraw-Hill; 1972.
- [30] Kakac S, Liu H. In: Stern RB, Didier D, Craig D, Esser C, editors. Heat exchangers selection, rating and thermal design. Boca Raton, Florida: CRC Press LLC; 1998. p. 57–61.
- [31] Forstner M, Hofmeister G, Joeller M, Dahl J, Braun M, Kleditzsch S, et al. CFD simulation of ash deposit formation in fixed bed biomass furnaces and boilers. Progress in Computational Fluid Dynamics 2006;6(4/5):248–61.
- [32] Traverso A, Magistri L, Scarpellini R, Massardo A. Demonstration plant and expected performance of an externally fired micro gas turbine for distributed power generation. In: Proceedings of ASME turbo expo 2003. ASME, editor. Paper GT2003-38268.
- [33] Lagerström G, Xie M. High performance & cost effective recuperatore for micro-gas turbines. In: Proceedings of ASME turbo expo 2002. ASME editor. Paper GT-2002-30402.
- [34] Traverso A, Massardo AF. Optimal design of compact recuperator for microturbine application. Applied Thermal Engineering 2005;25:2054–71.
- [35] Romier A. Small gas turbine technology. Applied Thermal Engineering 2004;24:1709–23.
- [36] Campanari S, Macchi E. Technical and tariff scenarios effect on microturbine trigenerative applications. ASME Journal of Engineering for Gas Turbines and Power 2004;126(3):581–9.

## Legends

- $\beta$ : compressor ratio  
 $\epsilon$ : kays efficacy  
 $\eta$ : efficiency  
 $\lambda$ : excess air ratio  
 $A$ : area, surface  
 $c_p$ : heat specific value  
 $C$ : heat capacity rate  
 $C^*$ : capacity rate ratio  
 $h$ : convection coefficient  
 $m$ : mass flow rate  
 $Nu$ : Nusselt number  
 $P$ : power  
 $Pr$ : Prandtl number  
 $Q$ : thermal, heat power  
 $Re$ : Reynolds number  
 $R$ : Biomass energy contribution  
 $T$ : Temperature  
 $TIT$ : Turbine Inlet Temperature  
 $TOT$ : Turbine Outlet Temperature  
 $U$ : Global heat exchange coefficient

## Subscripts

- bio*: biomass  
 $DT$ : Dry Ton  
 $e$ : electric  
 $i$ : inner side  
 $In$ : Input  
 $o$ : outer side  
 $m_{rid}$ : flow coefficient ( $m_{rid} = m \cdot T^{0.5} \cdot p^{-1}$ )  
 $max$ : maximum  
 $min$ : minimum  
 $pz$ : primary combustion zone  
 $rid$ : reduced mass flow rate  
 $th$ : thermal  
 $O$ : reference condition

## Abbreviations

- CS: Control System  
DCGT: Dual Combustion Gas Turbine

---

EFGT: Externally Fired Gas Turbine  
EGR: Exhaust Gas Recirculation  
GT: Gas Turbine  
HAGT: Hot Air Gas Turbine  
HE: Heat Exchanger  
HT: High Temperature

LCV: Lower Calorific Value (also LHV, Lower Heating Value)  
LHV: Lower Heating Value (also LCV, Lower Calorific Value)  
MGT: Micro Gas Turbine  
NG: Natural gas  
NTU: Number of Thermal Unit  
RPM: round per minute (rotational speed)